Cell-specific Bioorthogonal Tagging of Glycoproteins

Anna Cioce[a,b], Beatriz Calle[a,b], Tatiana Rizou[c,$], Sarah C. Lowery[d,$], Victoria Bridgeman[c,$], Keira E. Mahoney[d,$], Andrea Marchesi[a,b], Ganka Bineva-Todd[b], Helen Flynn[e], Zhen Li[a,b], Omur Y. Tastan[b], Chloe Roustan[f], Pablo Soro-Barrio[g], Mahmoud-Reza Rafiee[h], Acely Garza-Garcia[i], Aristotelis Antonopoulos[j], Thomas M. Wood[k,n], Tessa Keenan[l], Peter Both[m], Kun Huang[m,o], Fabio Parmeggiani[m,p], Ambrosius P. Snijders[e], Mark Skehel[e], Svend Kjaer[f], Martin A. Fascione[l], Carolyn R. Bertozzi[k], Stuart M. Haslam[j], Sabine Flitsch[m], Stacy A. Malaker[d], Ilaria Malanchi[c], Benjamin Schumann[a,b,*]

[a]Department of Chemistry, Imperial College London, 80 Wood Lane, W12 0BZ, London, United Kingdom.

[b]Chemical Glycobiology Laboratory, The Francis Crick Institute, 1 Midland Rd, NW1 1AT London, United Kingdom.

[c]Tumour-Host Interaction Laboratory, The Francis Crick Institute, 1 Midland Rd, NW1 1AT London, United Kingdom.

[d]Department of Chemistry, Yale University, 275 Prospect Street, New Haven, CT 06511, United States.

[e]Proteomics Science Technology Platform, The Francis Crick Institute, NW1 1AT London, United Kingdom.

[f]Structural Biology Science Technology Platform, The Francis Crick Institute, NW1 1AT London, United Kingdom.

[g]Bioinformatics & Biostatistics Science Technology Platform, The Francis Crick Institute, NW1 1AT London, United Kingdom.

[h]RNA Networks Laboratory, The Francis Crick Institute, 1 Midland Rd, NW1 1AT London, United Kingdom.

[i]Mycobacterial Metabolism and Antibiotic Research Laboratory, The Francis Crick Institute, 1 Midland Rd, NW1 1AT London, United Kingdom.

[j]Department of Life Sciences, Imperial College London, Exhibition Road, SW7 2AZ London, United Kingdom

[k]Department of Chemistry, Stanford University, 424 Santa Teresa St, Stanford, CA 94305, United States.

[l]Department of Chemistry, University of York, Heslington, YO10 5DD York, United Kingdom.

[m]Manchester School of Chemistry & Institute of Biotechnology, The University of Manchester, M1 7DN Manchester, United Kingdom.

[n]current address: Massachusetts Institute of Technology, 77 Massachusetts Ave, 02139 Cambridge, United States

[o]current address: Department of Chemistry and Biochemistry, University of Maryland, Baltimore, 620 W. Lexington St., Maryland 21250, United States.
[p]current address: Department of Chemistry, Materials and Chemical Engineering "G. Natta", Politecnico di Milano, Piazza Leonardo da Vinci 32, 20131 Milano, Italy

[$]These authors contributed equally.
*Correspondence should be addressed to: b.schumann@imperial.ac.uk.

ABSTRACT

Altered glycoprotein expression is an undisputed corollary of cancer development. Understanding these alterations is paramount but hampered by limitations underlying cellular model systems. For instance, the intricate interactions between tumour and host cannot be adequately recapitulated in monoculture of tumour-derived cell lines. More complex co-culture models usually rely on sorting procedures for proteome analyses and rarely capture the details of protein glycosylation. Here, we report a strategy termed Bio-Orthogonal Cell line-specific Tagging of Glycoproteins (BOCTAG). Cells are equipped by transfection with an artificial biosynthetic pathway that transforms bioorthogonally tagged sugars into the corresponding nucleotide-sugars. Only transfected cells incorporate bioorthogonal tags into glycoproteins in the presence of non-transfected cells. We employ BOCTAG as an imaging technique and to annotate cell-specific glycosylation sites in mass spectrometry-glycoproteomics. We demonstrate application in co-culture and mouse models, allowing for profiling of the glycoproteome as an important modulator of cellular function.

INTRODUCTION

Cancer is a multifactorial disease consisting of an interplay between host and tumour. Emulating the complexity of a tumour in cell monoculture is thus incomplete by design, requiring more elaborated co-culture systems or *in vivo* models.[1–3] Recent years have seen a stark increase in methods to probe the transcriptomes of tumour and host cell populations, respectively, providing some insight into their state within a multicellular conglomerate.[4] However, the relationship between transcriptome and proteome is still elusive.[5] In addition, posttranslational modifications (PTMs) heavily impact the plasticity of the proteome. Glycosylation is the most complex and most abundant PTM, but challenging to probe due to the non-templated nature of glycan biosynthesis.[6] Glycans are generated by the combinatorial interplay of >250 glycosyltransferases (GTs) and glycosidases, mostly in the secretory pathway.[7] A small number of glycoproteins aberrantly expressed in cancer, such as mucins, have been approved as diagnostic markers, but their discovery is a particular challenge.[8,9] This is especially true when *in vivo* or *in vitro* model systems comprise cell populations from the same organism that do not allow distinction of proteomes by amino acid sequence.[10,11] Methods to study the glycoproteome of a cell type in co-culture or *in vivo* are therefore an unmet need.

Metabolic oligosaccharide engineering (MOE) produces chemical reporters of glycan subtypes.[12] MOE reagents are membrane permeable monosaccharide precursors modified with chemical tags amenable to bioorthogonal chemistry.[13] Following incorporation into the glycoproteome, chemical tags are reacted with traceable enrichment handles or fluorophores, for instance by Cu(I)-catalysed azide-alkyne cycloaddition (CuAAC).[14,15] Many MOE reagents are based on analogues of sugars such as *N*-acetylgalactosamine (GalNAc) that are straightforward to chemically tag by replacing the acetamide with bioorthogonal *N*-acylamides (Fig. 1a). Unmodified GalNAc is normally activated by the biosynthetic GalNAc salvage pathway to the nucleotide-sugar UDP-GalNAc that can follow two major distinct metabolic fates (Fig. 1a).[14,16–18] First, the 20 members of the GalNAc transferase family (GalNAc-T1…T20) use UDP-GalNAc to form the linkage GalNAcα-Ser/Thr and thereby prime cancer-relevant O-GalNAc glycans.[14,19,20] Second, epimerisation at the GalNAc C4 position by the UDP-galactose-4-epimerase (GALE) yields UDP-*N*-acetylglucosamine (UDP-GlcNAc) that can be incorporated into different glycan subtypes, for instance Asn-linked N-glycans.[17,18,21] Certain chemical modifications at the *N*-acyl moiety can render GalNAc analogues recalcitrant to these metabolic processes. For instance, analogues of UDP-GalNAc with long alkyne-containing *N*-acyl substituents are not biosynthesised by the GalNAc salvage pathway and not used as substrates by wild type (WT)-GalNAc-Ts.[18,22–24] While being a substantial impediment to generating MOE reporters, we realised that overcoming these metabolic roadblocks might enable programmable bioorthogonal glycoprotein tagging. Such a strategy would allow for studying the glycoproteome in a cell-specific fashion, which is currently elusive despite the rapid advances in the development of new MOE reagents.

Here, we develop a technique called Bio-Orthogonal Cell-specific Tagging of Glycoproteins (BOCTAG). The strategy uses an artificial biosynthetic pathway to generate alkyne-tagged UDP-GalNAc and UDP-GlcNAc analogues from a readily available GalNAc precursor that is not accepted by the GalNAc salvage pathway. We find that a single methylene group between 5-carbon (GalNAlk) and 6-carbon (GalN6yne) *N*-acyl substituents drastically reduces uptake by the native GalNAc salvage pathway and thereby reduces the background of bioorthogonal labelling in non-transfected cells. Only cells carrying the artificial pathway biosynthesise the corresponding UDP-sugars (UDP-GalN6yne and UDP-GlcN6yne) that are then used by GTs to chemically tag the glycoproteome. We further expand the strategy with mutant GalNAc-Ts that are engineered to accept UDP-GalN6yne as a substrate. The combined use of an artificial biosynthetic pathway and engineered GalNAc-Ts enables GalN6yne-mediated fluorescent labelling of the cellular glycoproteome that is two orders of magnitude higher than in cells carrying neither component. We demonstrate that BOCTAG allows for programmable glycoprotein tagging in co-culture and mouse models. Moreover, the nature of the artificial biosynthetic pathway allowed for the use of readily available Ac_4GalN6yne as a precursor with enhanced stability over previously used caged GalN6yne-1-phosphates as an essential pre-requisite for *in vivo* applications. We show that the chemical modification enters a range of glycan subtypes, supporting the use of BOCTAG to tag a large number of glycoproteins in complex biological systems.

RESULTS

Developing an artificial biosynthetic pathway for chemically tagged UDP-sugars.

The human GalNAc salvage pathway consists of the kinase GALK2 and the pyrophosphorylases AGX1/2 to convert GalNAc first into GalNAc-1-phosphate and subsequently into UDP-GalNAc, respectively (Fig. 1a). Since neither analogue of GalNAc nor GalNAc-1-phosphate can be utilised by any other metabolic enzyme, the GalNAc salvage pathway was deemed suitable for monitoring conversions of each step while supplying readily accessible synthetic, bioorthogonal precursors. GALK2 and AGX1/2 are impervious to large chemical modifications at the *N*-acyl moiety of GalNAc (Fig. 1a), corroborated by crystal structures of these enzymes (Fig. S1).[18,24–26] An artificial biosynthetic pathway was thus designed to convert chemically tagged GalNAc analogues first to the corresponding sugar-1-phosphates and subsequently to the UDP-sugars. We chose both a 6-carbon hex-5-ynoate chain (GalN6yne) and a 5-carbon pent-4-ynoate chain (GalNAlk) as GalNAc modifications due to their availability and previous use by us and others.[18,24,27] In *in vitro* enzymatic assays detected by liquid chromatography-mass spectrometry (LC-MS), recombinant GALK2 accepted GalNAlk as a substrate, but only marginally accepted GalN6yne (Fig. 1b). In contrast, promiscuous bacterial *N*-acetylhexosaminyl kinases (NahK) from various source organisms converted GalN6yne to GalN6yne-1-phosphate almost quantitatively (Fig. 1b, Fig. S2a).[28] Similarly, the pyrophosphorylase AGX1 showed little to no turnover of both GalNAlk-1-phosphate and GalN6yne-1-phosphate to the corresponding UDP-sugars (Fig. 1b). We and others have mutated AGX1 at residue Phe383 to smaller amino acids to accommodate chemical *N*-acyl modifications.[24,29] $AGX1^{F383A}$, herein called mut-AGX1, converted both synthetic GalNAlk-1-phosphate and GalN6yne-1-phosphate to UDP-GalNAlk and UDP-GalN6yne, respectively (Fig. 1b).

We next assessed UDP-sugar biosynthesis in the living cell. Stable bicistronic expression of a codon-optimised version of *Bifidobacterium longum* NahK as well as mut-AGX1 in K-562 cells biosynthesised UDP-GalNAlk and UDP-GalN6yne from membrane-permeable per-acetylated precursors Ac_4GalNAlk and Ac_4GalN6yne, respectively (Fig. 1c). Expression of either enzyme alone or WT-AGX1 led to inefficient biosynthesis compared to levels of native UDP-sugars (Fig. S3). We confirmed these results by feeding cells a caged precursor of GalN6yne-1-phosphate that was uncaged in the living cell and converted to UDP-GalN6yne only in the presence of mut-AGX1 (Fig. S3). Alkyne-tagged UDP-GalNAc analogues were converted to the corresponding UDP-GlcNAc analogues (UDP-GlcNAlk or UDP-GlcN6yne, respectively) in cells by the epimerase GALE, which was corroborated in an *in vitro* epimerisation assay (Fig. 1a, c Fig. S2b, Fig. S3). Thus, installing an artificial biosynthetic pathway led to programmable biosynthesis of alkyne-tagged analogues of UDP-GalNAc and UDP-GlcNAc.

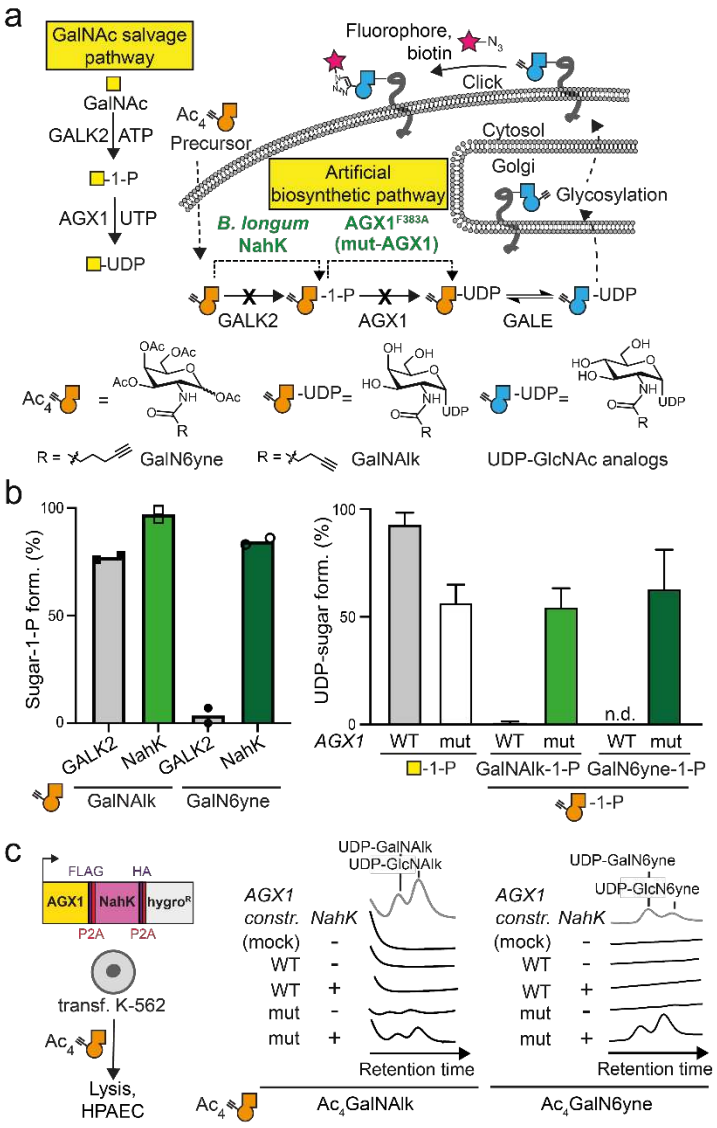

Fig. 1: Development of an artificial biosynthetic pathway for chemically tagged UDP-GalNAc/GlcNAc analogues. a, strategy of metabolic oligosaccharide engineering. A chemically modified GalNAc analogue that is not accepted by the GalNAc salvage pathway should be processed by an artificial biosynthetic pathway. *B. longum* NahK and mut-AGX1 biosynthesise UDP-GalNAc analogues and, by epimerisation, UDP-GlcNAc analogues. Incorporation into glycoconjugates can be traced by CuAAC. **b,** *in vitro* evaluation of GalNAc-1-phosphate analogue synthesis by human GALK2 or *B. longum* NahK (left) and UDP-GalNAc analogue synthesis by WT- or mut-AGX1 (right). Data were recorded in LC-MS assays and processed by integrated ion counts. Data are from two independent experiments and depicted as individual data points and means (left) or from three independent experiments and depicted as means + standard deviation (SD, right). **c,** biosynthesis of UDP-GalNAc/GlcNAc analogues in cells stably expressing both NahK and mut-AGX1 or either component, as assessed by high performance anion exchange chromatography (HPAEC). A hygromycin resistance gene allows for stable transfection. Data are representative of one out of two independent experiments collected on two different days. mock: pSBbi-GH empty plasmid.

We next assessed chemical tagging of the cell surface glycoproteome in living cells. K-562 cells stably expressing combinations of NahK and AGX1 were fed with DMSO, Ac_4GalNAlk or Ac_4GalN6yne and reacted with the clickable fluorophore CF680-picolyl azide by CuAAC. The MOE reagent Ac_4ManAlk that enters the pool of the sugar sialic acid was included as a positive control. Alkyne tags were visualised by in-gel fluorescence after cell lysis (Fig. 2a). While Ac_4GalNAlk feeding led to high-intensity fluorescent signal when NahK and mut-AGX1 were expressed, substantial signal was observed in cells expressing WT-AGX1 when NahK was present (Fig. 2a). Fluorescent signal after Ac_4GalNAlk feeding was also observed in cells transfected with an empty plasmid or only overexpressing WT-AGX1, confirming the permissiveness of the GalNAc salvage pathway for GalNAlk (Fig. 1b).[18] In contrast, Ac_4GalN6yne incorporation was critically dependent on the expression of mut-AGX1, while the presence of NahK led to a further sixfold increase in fluorescence intensity (Fig. 2a). Ac_4ManAlk gave fluorescent signal regardless of the enzyme combination expressed. Dose response experiments showed that Ac_4GalN6yne-mediated fluorescence intensity increased over two orders of magnitude with the concentration of the probe between 16 nM and 50 μM only when NahK and mut-AGX1 were present (Fig. 2b). Transfection and feeding with chemically modified sugars can in theory alter the cellular transcriptome, leading to artefacts in protein expression and metabolic labelling. We performed transcriptomic analyses in cells transfected with either NahK/mut-AGX1 or empty plasmid, and fed with either DMSO vehicle, Ac_4GalN6yne or Ac_4GalNAc. By performing correlation plot and principal component analysis (PCA, Fig. S4), we observed that the day of sample collection has a greater effect on transcript levels than either transgene expression or compound treatment (Fig. S4b). These data suggest that neither artificial biosynthetic pathway nor compound feeding has substantial effects on the transcriptome. We further measured the levels of endogenous UDP-sugars and found no substantial changes upon expression of mut-AGX1, regardless of feeding withDMSO or Ac_4GalN6yne. Similarly, expression of NahK and mut-AGX1 led to no changes when fed with Ac_4GalN6yne (Fig. S5a). Levels of UDP-GlcNAc/GalNAc were increased by 33/36%, 28/30%, and 26/30% in WT-AGX1 and DMSO-fed NahK/mut-AGX1 respectively. The relative ratio of both metabolites was constant in all cell lines (Fig. S5b). We also found no differences in concentrations of the metabolite cytidine monophosphate-*N*-acetylneuraminic acid (CMP-Neu5Ac). To assess if the cellular glycome would be affected by variations in nucleotide-sugar concentrations, we performed lectin blotting on lysates of cell expressing NahK/mut-AGX1. We found no differences in binding patterns of four lectins as well as the antibody RL2 detecting nucleocytoplasmic O-linked GlcNAc compared to mock-transfected cells (Fig. S6). We also established that chemical tagging is measurable in a dose-dependent fashion both on the cell surface (when CuAAC was performed prior to lysis) and in lysate (Fig. S7). Due to the robustness of metabolic incorporation, we used Ac_4GalN6yne as an MOE reagent for all subsequent applications of BOCTAG.

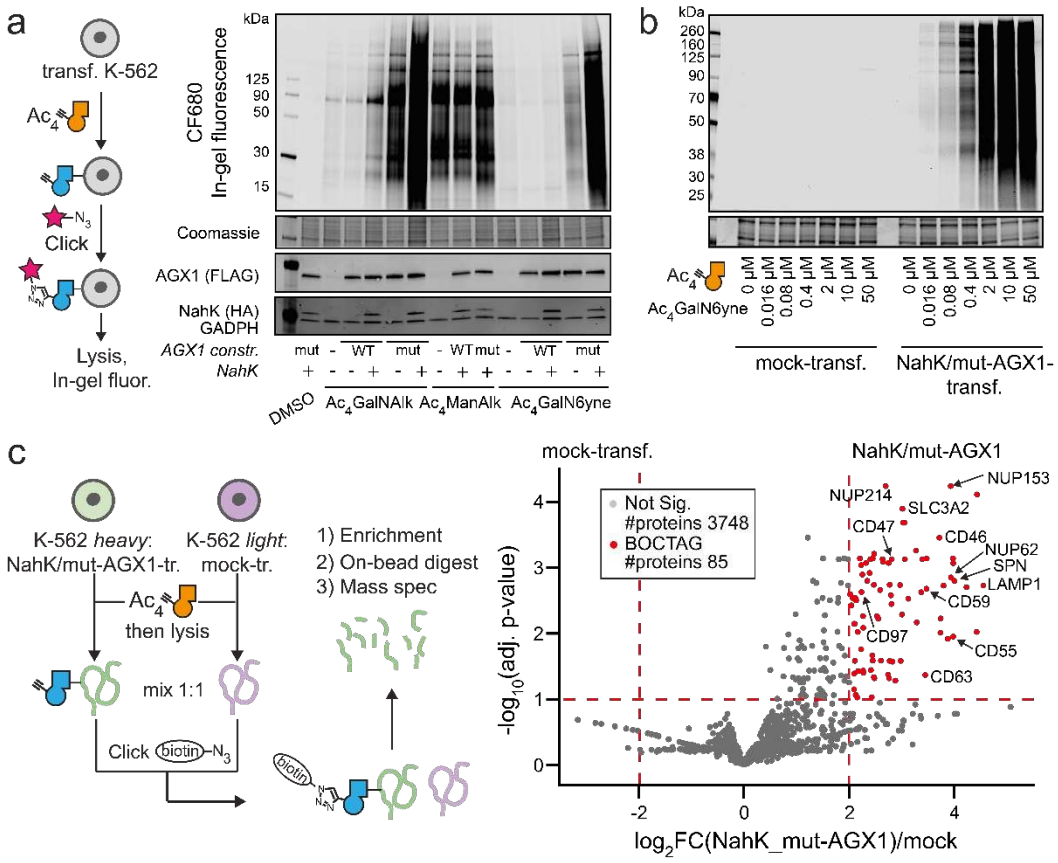

Fig. 2: An artificial biosynthetic pathway enables programmable chemical tagging of the glycoproteome. **a,** evaluation of cell surface glycoproteome tagging after treating K-562 cells stably expressing NahK/AGX1 combinations with 50 µM Ac_4GalNAlk, 50 µM Ac_4GalN6yne or 10 µM Ac_4ManNAlk. Glycoproteins were visualised by in-gel fluorescence after treating cells with CF680-picolyl azide under CuAAC conditions and subsequent cell lysis. **b,** dose-response experiment of cell surface glycoproteome tagging, with samples processed as in **a**. Data in **a** and **b** are representative of one out of two independent experiments. **c,** quantitative measurement of glycoprotein tagging by SILAC. Data were analysed from three independent experiments, collected on three different days, with forward (heavy mock, light NahK/mut-AGX1) and reverse (light mock, heavy NahK/mut-AGX1) analyses incorporated as a total of six replicates. Data are visualised as volcano plot, choosing 4-fold enrichment and a p-value of 0.1 as cut-offs, with example glycoproteins annotated. Significance levels were indicated. Mock: pSBbi-GH empty plasmid.

An artificial biosynthetic pathway allows for programmable enrichment of the glycoproteome.

We used Stable Isotope Labelling by Amino Acids in Cell Culture (SILAC)-based proteome analysis to confirm and quantify chemical glycoproteome tagging. K-562 cells transfected with NahK/mut-AGX1 or an empty plasmid (mock-transfected). Both were individually grown in heavy or light media in the presence of either Ac_4GalN6yne or DMSO. Lysates of these cells were mixed as different combinations to contain equal amounts of heavy and light protein, and clickable biotin-picolyl azide was installed on tagged glycoproteins by CuAAC. Enrichment on neutravidin beads followed by on-bead digest allowed analysis by quantitative mass

spectrometry (MS). In three independent experiments in which both combinations of heavy and light SILAC labelling each were used (Fig. 2c), we found peptides from 85 proteins to be significantly enriched in NahK/mut-AGX1-transfected cells (Supplementary Table 1). More than 99% (84/85) of these proteins have been previously annotated[30–32] as either N- or O-glycosylated, including the nucleoporins Nup62 and Nup153 and the cell surface proteins CD47 and NOTCH1, confirming the stringency of the approach for tagging glycoproteins.

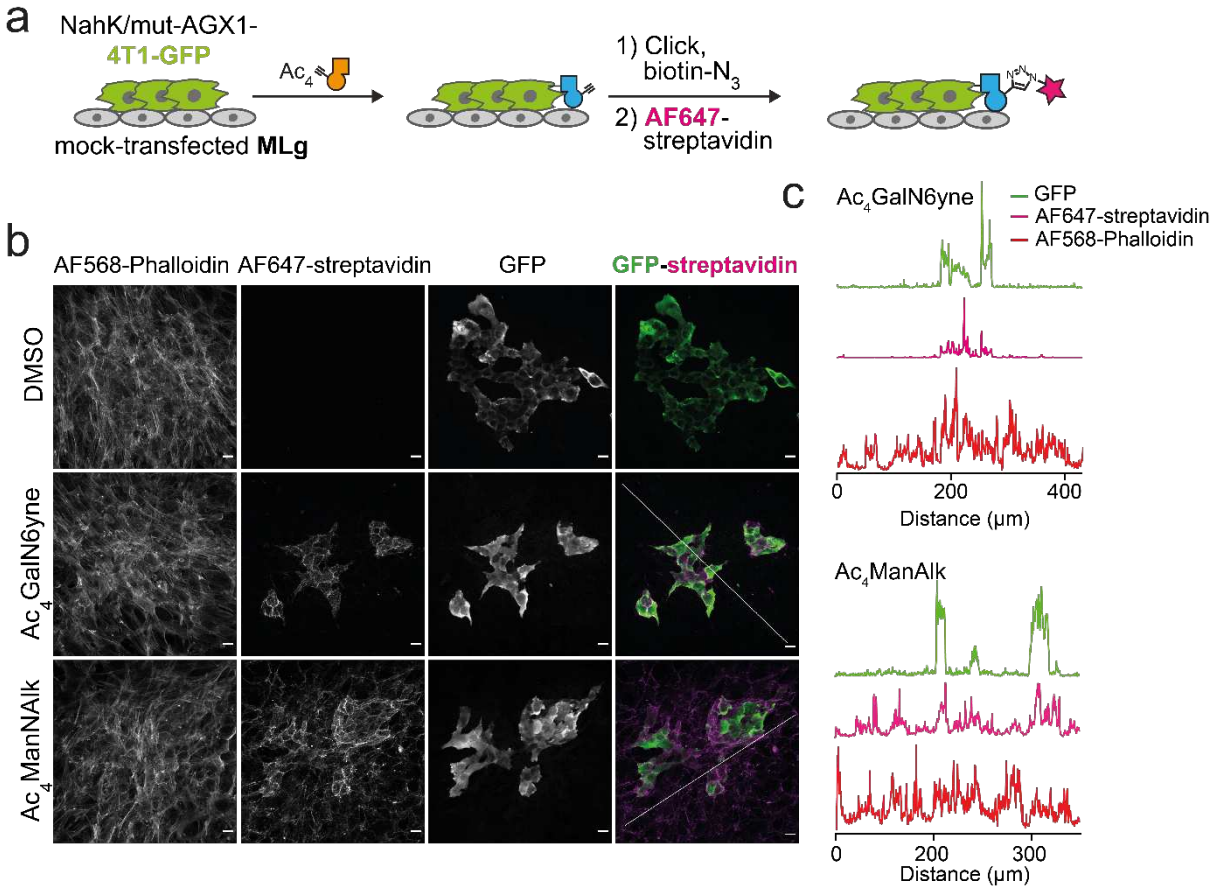

Fig. 3: Bioorthogonal cell-specific glycoprotein tagging in co-culture. a, schematic of the 4T1-MLg co-culture experiment. Green fluorescent protein (GFP)-expressing 4T1 cells transfected with NahK/mut-AGX1 should be selectively positive for Alexafluor647-labelling in BOCTAG. **b,** fluorescence microscopy, using co-cultures fed with 50 µM Ac4GalN6yne or 50 µM Ac4ManNAlk as well as Alexafluor568-phalloidin as a counterstain. Scale bar, 20 µm. **c**, intensity profile of fluorescent signal between GFP and AF647 in Ac4GalN6yne- (top) or Ac4ManNAlk-fed (bottom) co-cultures. The intensity profile of GFP, AF647-Streptavidin and AF568-Phalloidin signals was measured along a diagonal line drawn along the fluorescent image. Data are representative of one out of two independent experiments.

Cell type-specific glycoproteome tagging in co-culture.

We next assessed the suitability of the artificial biosynthetic pathway NahK/mut-AGX1 as a BOCTAG cell type-specific glycoproteome labelling technique by fluorescence microscopy. Colonies of NahK/mut-AGX1-

transfected and GFP-expressing 4T1 breast cancer cells were established on a monolayer of non-transfected MLg fibroblast cells by co-culturing for 72 h before media supplementation with either Ac_4GalN6yne, Ac_4ManAlk or DMSO (Fig. 3a). Clickable biotin-picolyl azide was installed by CuAAC followed by Streptavidin-AF647 staining to visualise chemical tagging, and cells were counter-stained with fluorescently labelled phalloidin. Streptavidin-AF647 signal was strongly and reproducibly restricted to GFP-expressing cells only when Ac_4GalN6yne was fed and NahK/mut-AGX1 were expressed (Fig. 3b, c, Fig. S8-S11), indicating a localised BOCTAG signal. In contrast, the promiscuous MOE reagent Ac_4ManNAlk was non-specifically incorporated throughout the entire co-culture (Fig. 3b, c, Fig. S8-S11). When both GFP-4T1 and MLg cell lines expressed NahK/mut-AGX1 were fed with Ac_4GalN6yne, both exhibited a strong Streptavidin-AF647 signal (Fig. S11b). Taken together, BOCTAG enables cell-specific tagging of cell surface glycoproteins in co-culture.

Assessing and manipulating the glycan types tagged by GalN6yne.

We next sought to assess and expand the glycan subtypes targeted by our MOE approach. We were prompted by our recent findings that GalNAc analogues with bulky *N*-acyl chains such as GalN6yne are not incorporated into O-GalNAc glycans by WT-GalNAc-Ts (Fig. 4a).[23,24,33] We have created GalNAc-T mutants termed BH-GalNAc-Ts (for "bump-and-hole engineering", the process used to design the mutants) that selectively use such chemically tagged UDP-GalNAc analogues in glycosylation reactions.[23,24,33] We stably co-expressed WT- or BH-versions of GalNAc-T1 or T2 from plasmids also encoding NahK and mut-AGX1 in K-562 cells (Fig. 4a). Expression of BH-GalNAc-Ts increased the intensity of in-gel fluorescence more than sevenfold over expression of WT-GalNAc-Ts when cells were fed with Ac_4GalN6yne (Fig. 4b). WT-AGX1 expressing cells lacked UDP-GalN6yne/UDP-GlcN6yne biosynthesis and did not show any discernible fluorescent signal over vehicle control DMSO (Fig. 1c). We assessed the subtypes of the chemically tagged glycans by digestion with the hydrolytic enzymes PNGase F (reduces N-glycosylation), StcE (digests mucin-type glycoproteins) and OpeRATOR (digests O-GalNAc glycoproteins in the presence of the sialidase SialEXO) prior to in-gel fluorescence.[34] In cells expressing NahK, mut-AGX1 and WT-GalNAc-Ts, fluorescent labelling was sensitive to PNGase F treatment, indicating that the major target structures are N-glycoproteins in these cells (Fig. 4c). Incomplete signal abrogation of signal by PNGase F could result from incorporation of GlcN6yne in the protein-proximal core of N-linked glycans, which would be functionalised with fluorophore before digest. Co-expression of BH-GalNAc-Ts led to additional highly intense fluorescent signal of a small number of O-glycoproteins with sensitivity to both StcE and OpeRATOR/SialEXO (Fig. 4c). Thus, BH-GalNAc-Ts broaden the target scope of chemical tagging to include O-GalNAc glycoproteins with high incorporation efficiency. In accordance with this finding, we performed quantitative MS-proteome analysis by SILAC of cell lines expressing NahK/mut-AGX1/BH-GalNAc-T2 (BH-T2). In contrast to cells expressing only NahK/mut-AGX1/WT-T2 (Fig. 2c), we observed an increase from 50% to 61% of previously annotated O-GalNAc glycoproteins in the enriched protein fraction (Supplementary Table 1).[30–32] Concomitant with GalN6yne incorporation into the O-GalNAc glycoproteome, we found a relative reduction of certain glycans containing 2,3-linked sialic acid upon BH-GalNAc-T2 expression in lectin blot analysis (Fig. S12-13) and by mass spectrometry (Fig. S14-15). Using a doxycycline-inducible expression system,[24] we confirmed this tendency with WT-GalNAc-T2 in a titratable fashion (Fig. S13). Taken together, overexpression of BH-GalNAc-Ts

increases incorporation of chemically tagged glycans by BOCTAG by an order of magnitude, allowing entry into the O-GalNAc glycoproteome.

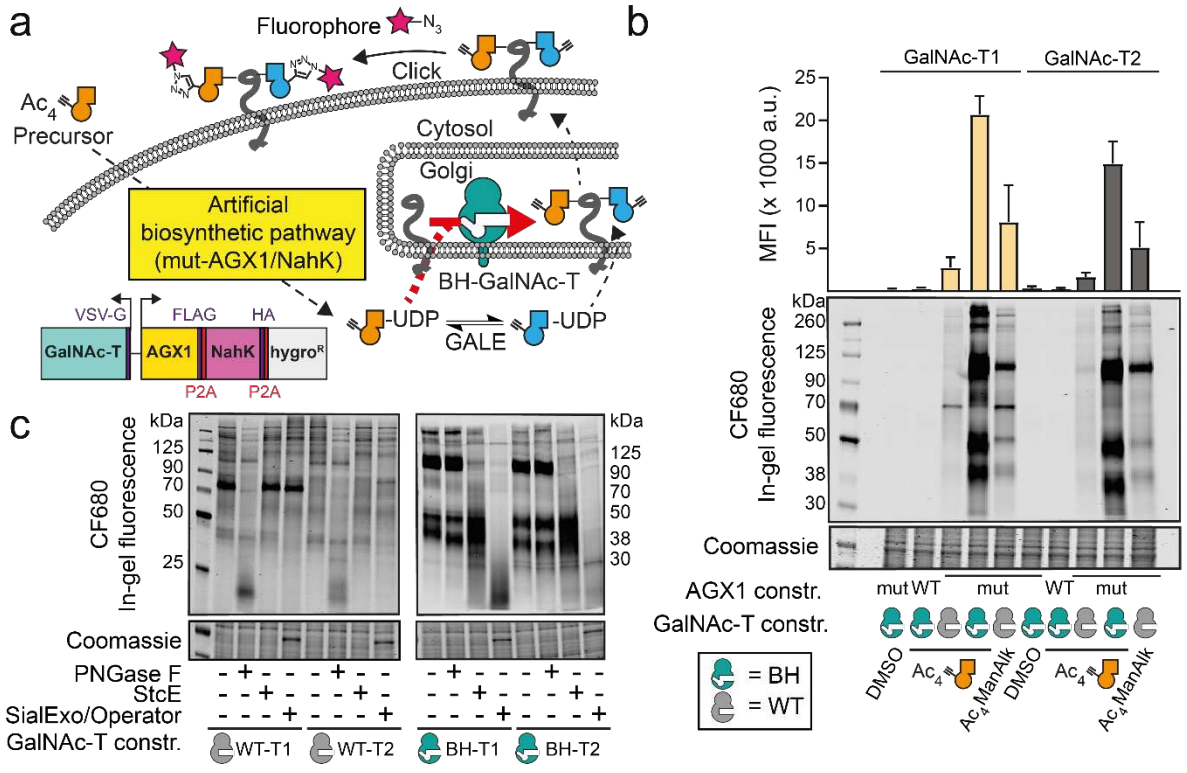

Fig. 4: Enhancement of programmable glycoprotein tagging by expression of BH-GalNAc-Ts. a, strategy of expanding glycoprotein tagging to include O-GalNAc glycans. Expression of BH-GalNAc-Ts selectively engineered to accommodate bulky chemical tags enhances O-GalNAc tagging in cells expressing NahK/mut-AGX1. **b,** evaluation of tagging efficiency by feeding transfected K-562 cells with either DMSO, 1 μM Ac_4GalN6yne or 2 μM Ac_4ManNAlk. Tagging was analysed by in-gel fluorescence and quantification by densitometry as means + SD from three independent experiments. **c,** assessment of tagged glycan subtypes by treating the samples of cells fed with Ac_4GalN6yne analysed in **b** with hydrolytic enzymes. Lysates of WT- and BH-GalNAc-T1/T2 transfected cells are loaded on two different gels. Gel images are shown with different intensities to best visualise the effect of enzyme treatment. Data are representative of one out of a total of four replicate labelling experiments performed on two different days.

MS-based validation of cell-type specific labelling in co-culture models.

We then validated BOCTAG as a strategy for cell-specific MS-glycoproteome analysis. We chose a co-culture model between murine 4T1 and human MCF7 breast cancer cell lines, opting to distinguish labelled glycoproteins with species-specific peptide sequences by label-free quantitative (LFQ) LC/MS-MS analysis. We transfected cells with either NahK/mut-AGX1/BH-GalNAc-T2 (termed “BOCTAG-T2”) or empty plasmid (pSBbi-Hyg, mock), co-cultured murine and human cells overnight and subsequently fed the co-cultures with either Ac_4GalN6yne or vehicle DMSO. Chemically tagged glycoproteins in the secretome were reacted with acid-cleavable biotin-picolyl azide by CuAAC and enriched on neutravidin magnetic beads (Fig. 5a). On-bead

digest yielded a peptide fraction and left glycopeptides bound to beads to be separately eluted with formic acid[24,35,36]. Peptide samples were assessed by LFQ MS-proteomics in two independent experiments, choosing an 8-fold enrichment and a p-value of 0.1 as cut-offs. We observed species-specific protein enrichment: BOCTAG-T2-expressing 4T1 cells led to 132 selectively enriched murine peptides while BOCTAG-T2-expressing MCF7 cells allowed detection of 24 selectively enriched human peptides when co-cultured with mock-transfected cells of the respective other species (Fig. 5b, Supplementary Table 2). Only two human peptides and one murine peptide were found in the enriched datasets from the corresponding other species.

BOCTAG-T2 allows for cell-specific glycosylation site identification. Using a tandem MS technique consisting of higher energy collision dissociation (HCD)-triggered electron transfer dissociation (ETD), we identified 37 specific glycosylation sites on 57 murine glycopeptides from 4T1 cells and 9 specific glycosylation sites on 12 human glycopeptides from MCF7 cells in secretome samples (Fig. 5c, Supplementary Table 2). Our data indicated glycosylation of homologous glycopeptides from murine and human origins in pro-X carboxypeptidase in secretome (Fig. 5d, Fig. S16). We also performed an MS-glycoproteomics experiment in lysate from the 4T1/MCF7 co-culture expressing BOCTAG-T2 or empty plasmid. We annotated a total of 4 specific glycosylation sites on 11 murine glycopeptides from 4T1 samples and 2 specific glycosylation sites on 8 human glycopeptides from MCF7 cells (Supplementary Table 3). Particularly, we identified a homologous glycopeptide from both human and murine glucosidase 2 (Fig. S17). The presence of the chemical tag facilitated manual annotation of mass spectra in all cases due to the specific mass shift associated with the chemical modification, in line with our previous results.[37]

Bioorthogonal cell-specific tagging of glycoproteins in *vivo.*

We next investigated the applicability of our BOCTAG strategy in an *in vivo* tumour model. Tumours were grown in the fat pads of NOD-SCID IL2Rgnull (NSG) mice, consisting of 4T1 cells expressing GFP and either BOCTAG-T2 (one fat pad) or no additional transgene (empty plasmid, another fat pad). These mice were intraperitoneally injected with Ac_4GalN6yne, vehicle or Ac_4MAnNAlk once daily for five consecutive days (Fig. 5e). At the end of the treatment, the tumours were harvested, homogenised, treated with biotin-picolyl azide under CuAAC conditions and the labelling analysed by streptavidin blot. A strong fluorescent signal was observed in the BOCTAG-T2 tumours treated with Ac_4GalN6yne (Fig 5e). In contrast, tumours transfected with empty plasmid showed minimal labelling signal with either vehicle or Ac_4GalN6yne treatment. All samples treated with Ac_4ManNAlk irrespective of the presence of NahK/mut-AGX1/BH-T2 displayed strong fluorescent signal. These data demonstrated that glycoproteins are selectively tagged when NahK/mut-AGX1/BH-T2 are expressed in the tumour. We also performed intratumoral injections of either Ac_4GalN6yne or DMSO and observed the same BOCTAG-T2-dependent labelling (Fig. S18a).

To evaluate the protein expression levels of NahK/mut-AGX1/BH-T2 *ex vivo*, part of the tumours was digested, plated and cells cultured. Protein expression of NahK/mut-AGX1/BH-T2 was assessed by Western blot and found to be comparable to expression levels before *in vivo* injection (Fig. S18b). Cells also generally retained the ability to incorporate Ac4GalN6yne-dependent chemical glycoproteome tagging (Fig. S18b).

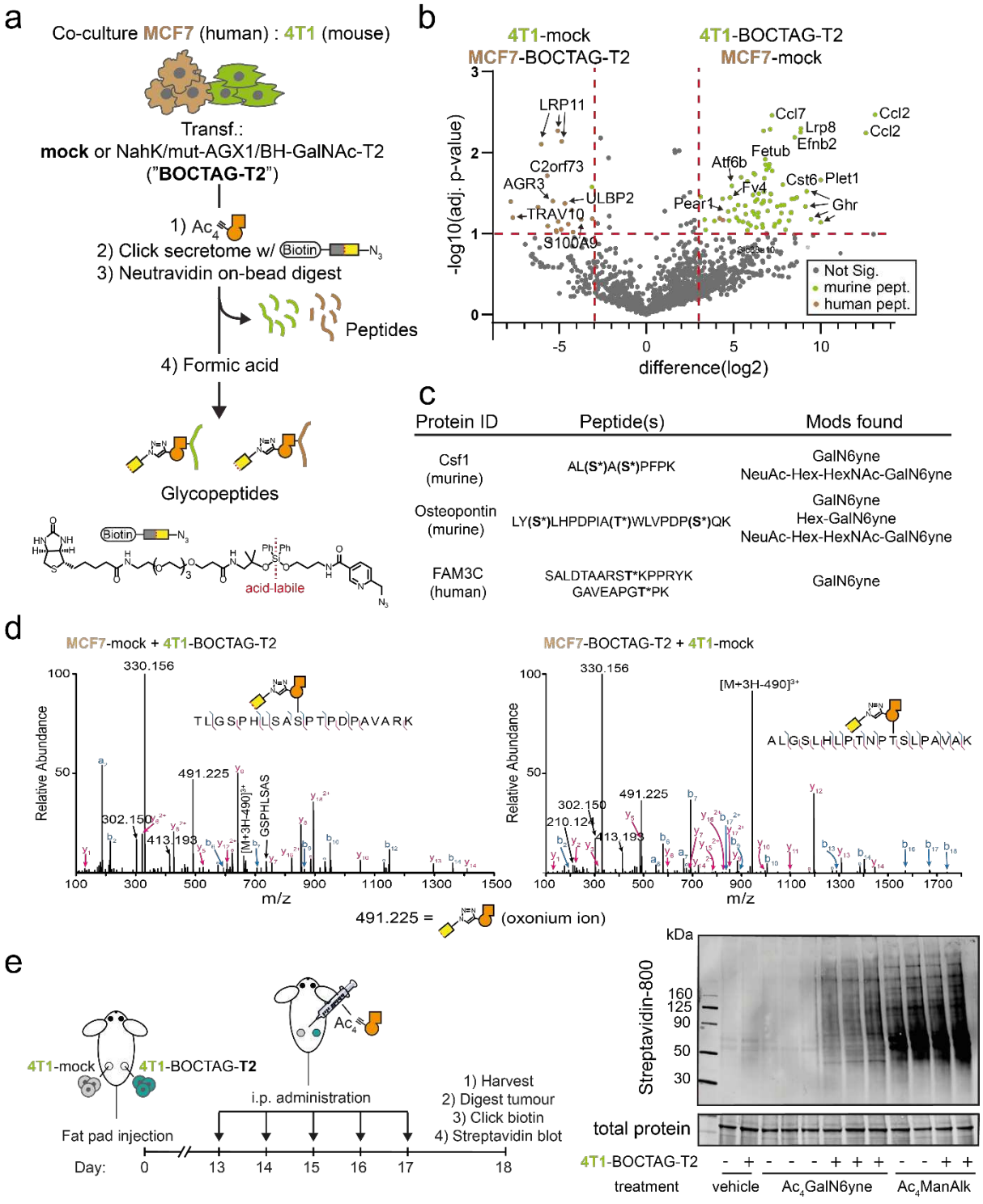

Fig. 5: BOCTAG labels glycoproteins in a cell-specific manner in co-culture and *in vivo*. a, cell-selective enrichment and MS-glycoproteome analysis of murine-human co-culture systems. MCF7 and 4T1 cells transfected as indicated were co-cultured overnight and treated with DMSO or 10 µM Ac_4GalN6yne for 24h. Secretome was subjected to CuAAC with acid-cleavable biotin-picolyl azide and enriched on neutravidin beads. On-bead digest yielded peptide fractions while acid treatment of beads yielded glycopeptide fractions. **b,** MS analysis of peptide fractions from **a** by choosing 8-fold enrichment and a p-value of 0.1 as cut-offs. Species-specific peptides are indicated. Data are from two independent experiments. **c,** examples of enriched

glycopeptides and glycoforms. Asterisk annotates glycosylation sites; parentheses indicate potential glycosylation sites that could not be confidently assigned. **d,** HCD spectra of homologous glycopeptides from murine (left) and human (right) origins. Peptide sequences were confirmed by ETD (Fig S16). **e,** *in vivo* glycoproteome tagging by BOCTAG-T2. Tumours were grown in fat pads of mice as described. BOCTAG-T2 and mock tumours were grown in the same mouse treated systemically by intraperitoneal (i.p. administration) for five days with 200 mg/kg Ac_4GalN6yne, Ac_4ManNAlk or the corresponding volume of vehicle. Tumours were harvested, lysed, subjected to CuAAC with biotin-picolyl azide and analysed by streptavidin blot. Hex = Hexose, e.g. galactose; NeuAc = *N*-acetylneuraminic acid; HexNAc = *N*-acetylhexosamine, e.g. GlcNAc. mock: pSBbi-Hyg.

DISCUSSION

We developed BOCTAG to address two major shortcomings in the biosciences. First, there is still an unmet need for characterising proteins produced by a particular cell type. Glycans are a means to an end in this respect, and the large signal-to-noise ratio in our fluorescent labelling experiments indicates that BOCTAG allows for efficient protein tagging. The approach is complementary to other techniques, including the use of unnatural amino acids, proximity biotinylation and ligand-targeting delivery approaches.[38,39,40] Second, directly incorporating glycans in the analysis will give insight into cell-type-specific glycosylation sites and possibly glycan structures to add another dimension to proteome profiling. We have shown that BOCTAG allows incorporation into N-, O-GalNAc linked glycans. We note that chemical tagging of intracellular O-GlcNAc glycans is likely,[41] and welcome incorporation into as many glycan types as possible. The presence of a modification that can be observed by MS as a direct corollary of chemical tools allows for further validation of enriched glycoproteins, facilitating glycoproteome analysis even in complex co-culture or *in vivo* settings. An artificial biosynthetic pathway was essential to ensure minimal background labelling while being able to supply the tagged sugar as an easy-to-synthesise MOE reagent. To this end, the use of the kinase NahK allows for use of a per-acetylated bioorthogonal sugar that is fundamental to *in vivo* use and in marked difference to highly unstable caged sugar-1-phosphates used previously.[19,24] To enable BOCTAG, cells require transfection with at least two transgenes. However, the design of a multicistronic, transposase-responsive plasmid ensures that transfection efforts are straightforward.[42,43] BOCTAG allowed us to selectively tag tumour glycoproteomes *in vivo*, highlighting the robustness of the approach. MOE reagents have been chemically caged to be released by enzymes overexpressed in cancer.[44–46] While independent of transfection, such targeting can be accompanied by substantial background labelling in non-cancerous tissue. BOCTAG allows for programmable glycoprotein tagging with remarkable signal-to-noise ratio, and an enabling technology that will transform our understanding of tumour-host interactions particularly in the context of protein glycosylation.

Data availability

Mass spectrometry proteomics and glycoproteomics data are available at http://www.ebi.ac.uk/pride with identifiers PXD035430, PXD035437, PXD035438, PXD035445 and PXD035449.

ACKNOWLEDGEMENTS

We thank Kayvon Pedram for providing StcE and Junwon Choi for UDP-sugar standards for chromatography. We thank Lucia Di Vagno for help with glycoproteomics data, Phil Walker for advice on vector choice, and Rocco D'Antuono of the Crick Advanced Light Microscopy STP for support and assistance in this work. We thank Jerome Nicod, Robert Goldstone and Phil East of the of the Advanced Sequencing Facility and Bioinformatics and Biostatistics Science Technology Platform for help with transcriptomics samples preparation, sequencing and data analysis. We are grateful for support by the Francis Crick Institute Cell Services and Peptide Chemistry Science Technology Platforms. This work was supported by the Francis Crick Institute (A. C., B. C., T. R., V. B., A. M., G. B.-T., H. F., Z. L., O. Y. T., C. R., P. S.-B., S. K., I. M., B. S.) which receives its core funding from Cancer Research UK (FC001749, FC001045), the UK Medical Research Council (FC001749, FC001045) and Wellcome Trust (FC001749, FC001045). This work was supported by the ERC (788231 to S. L. F.), the Wellcome Trust (218304/Z/19/Z to A. M. and B. S.). the EPSRC (EP/S013741/1 to T. K. and M. A. F., and EP/S005226/1 to S. L. F.), the BBSRC (BB/T01279X/1 to Z. L. and B. S., BB/M027791/1 and BB/M028836/1 to S. L. F., and BB/M02847X/1 to T. K. and M. A. F.) and the NIH (R01 CA200423 to C.R.B.). B.C. was supported by a Crick-HEI studentship funded by the Department of Chemistry at Imperial College London and the Francis Crick Institute. S. A. M. is supported by the Yale Science Development Fund and NIGMS R35 GM147039. K. E. M. is supported by a Yale Endowed Postdoctoral Fellowship by the National Instituted if Health Chemical Biology Training Grant (T32 GM067543). For the purpose of Open Access, the author has applied a CC BY public copyright licence to any Author Accepted Manuscript version arising from this submission.

392 REFERENCES

393 1. Ombrato, L. *et al.* Metastatic-niche labelling reveals parenchymal cells with stem features.
394 *Nature* **572**, 603–608 (2019).

395 2. del Pozo Martin, Y. *et al.* Mesenchymal Cancer Cell-Stroma Crosstalk Promotes Niche
396 Activation, Epithelial Reversion, and Metastatic Colonization. *Cell Rep.* **13**, 2456–2469
397 (2015).

398 3. Yamaguchi, H. & Sakai, R. Direct interaction between carcinoma cells and cancer associated
399 fibroblasts for the regulation of cancer invasion. *Cancers (Basel).* **7**, 2054–2062 (2015).

400 4. Nayak, R. & Hasija, Y. A hitchhiker's guide to single-cell transcriptomics and data analysis
401 pipelines. *Genomics* **113**, 606–619 (2021).

402 5. Schoof, E. M. *et al.* Quantitative single-cell proteomics as a tool to characterize cellular
403 hierarchies. *Nat. Commun.* **12** (2021).

404 6. Varki, A. & Gagneux, P. Biological Functions of Glycans. in *Essentials of Glycobiology, 3rd*
405 *edition* (2017).

406 7. Clausen, H., Schjoldager, K. T., Narimatsu, Y., Joshi, H. J. & Clausen, H. Global view of
407 human protein glycosylation pathways and functions. *Nat. Rev. Mol. Cell Biol.* **21**, 729–749
408 (2020).

409 8. Kailemia, M. J., Park, D. & Lebrilla, C. B. Glycans and glycoproteins as specific biomarkers
410 for cancer. *Anal. Bioanal. Chem.* **409**, 395–410 (2017).

411 9. Scott, E. & Munkley, J. Glycans as biomarkers in prostate cancer. *Int. J. Mol. Sci.* **20**, (2019).

412 10. Krasny, L. & Huang, P. H. Data-independent acquisition mass spectrometry (DIA-MS) for
413 proteomic applications in oncology. *Mol. Omics* **17**, 29-42 (2021).

414 11. Gauthier, N. P. *et al.* Cell-selective labeling using amino acid precursors for proteomic studies
415 of multicellular environments. *Nat. Methods* **10**, 768–773 (2013).

416 12. Sletten, E. M. & Bertozzi, C. R. Bioorthogonal chemistry: Fishing for selectivity in a sea of
417 functionality. *Angew. Chem. Int. Ed.* **48**, 6974–6998 (2009).

418 13. Parker, C. G. & Pratt, M. R. Click Chemistry in Proteomic Investigations. *Cell* **180**, 605–632
419 (2020).

420 14. Hang, H. C., Yu, C., Kato, D. L. & Bertozzi, C. R. A metabolic labeling approach toward
421 proteomic analysis of mucin-type O-linked glycosylation. *Proc. Natl. Acad. Sci. U. S. A.* **100**,
422 14846–14851 (2003).

15. Besanceney-Webler, C. *et al.* Increasing the efficacy of bioorthogonal click reactions for bioconjugation: A comparative study. *Angew. Chem. Int. Ed.* **50**, 8051–8056 (2011).

16. Zaro, B. W., Yang, Y., Hang, H. C. & Pratt, M. R. Chemical reporters for fluorescent detection and identification of O-GlcNAc-modified proteins reveal glycosylation of the ubiquitin ligase NEDD4-1. *Proc. Natl Acad. Sci. U. S. A.* **108**, 1–6 (2011).

17. Boyce, M. *et al.* Metabolic cross-talk allows labeling of O-linked β-N- acetylglucosamine-modified proteins via the N-acetylgalactosamine salvage pathway. *Proc. Natl. Acad. Sci. U. S. A.* **108**, 3141–3146 (2011).

18. Cioce, A. *et al.* Optimization of Metabolic Oligosaccharide Engineering with Ac4GalNAlk and Ac4GlcNAlk by an Engineered Pyrophosphorylase1. Cioce, A. et al. Optimization of Metabolic Oligosaccharide Engineering with Ac4GalNAlk and Ac4GlcNAlk by an Engineered Pyrophosphorylase. *ACS Chem. Biol.* **16***,* 1961–1967 (2021).

19. Debets, M. F. *et al.* Metabolic precision labeling enables selective probing of O-linked N -acetylgalactosamine glycosylation . *Proc. Natl. Acad. Sci U. S. A.*. **117**, 25293–25301 (2020).

20. Pratt, M. R. *et al.* Deconvoluting the functions of polypeptide N-α-acetylgalactosaminyltransferase family members by glycopeptide substrate profiling. *Chem. Biol.* **11**, 1009–1016 (2004).

21. Broussard, A. *et al.* Human UDP-galactose 4′-epimerase (GALE) is required for cell-surface glycome structure and function. *J. Biol. Chem.* **295**, 1225–1239 (2020).

22. Kingsley, D. M. *et al.* Reversible defects in O-linked glycosylation and LDL receptor expression in a UDP-Gal/UDP-GalNAc 4-epimerase deficient mutant. *Cell* **44**, 749-759 (1986).

23. Choi, J. *et al.* Engineering Orthogonal Polypeptide GalNAc-Transferase and UDP-Sugar Pairs. *J. Am. Chem. Soc.* **141**, 13442–13453 (2019).

24. Schumann, B. *et al.* Bump-and-Hole Engineering Identifies Specific Substrates of Glycosyltransferases in Living Cells. *Mol. Cell* **78**, 824-834.e15 (2020).

25. Pouilly, S., Bourgeaux, V., Piller, F. & Piller, V. Evaluation of analogues of GalNAc as substrates for enzymes of the Mammalian GalNAc salvage pathway. *ACS Chem. Biol.* **7**, 753–760 (2012).

26. Bourgeaux, V., Piller, F. & Piller, V. Two-step enzymatic synthesis of UDP-N-acetylgalactosamine. *Bioorg. Med. Chem. Lett.* **15**, 5459–5462 (2005).

27. Lewis, Y. E. *et al.* O-GlcNAcylation of α-Synuclein at Serine 87 Reduces Aggregation

without Affecting Membrane Binding. *ACS Chem. Biol.* **12**, 1020–1027 (2017).

28. Keenan, T. *et al.* Profiling Substrate Promiscuity of Wild-Type Sugar Kinases for Multi-fluorinated Monosaccharides. *Cell Chem. Biol.* **27**, 1199-1206.e5 (2020).

29. Yu, S. *et al.* Metabolic labeling enables selective photocrosslinking of O-GlcNAc-modified proteins to their binding partners. *Proc. Natl Acad. Sci. U. S. A.* **109**, 1–6 (2012).

30. York, W. S. *et al.* GlyGen: Computational and Informatics Resources for Glycoscience. *Glycobiology* **30**, 72–73 (2020).

31. Steentoft, C. *et al.* Precision mapping of the human O-GalNAc glycoproteome through SimpleCell technology. *EMBO J.* **32**, 1478–1488 (2013).

32. Joshi, H. J. *et al.* GlycoDomainViewer: a bioinformatics tool for contextual exploration of glycoproteomes. *Glycobiology* **28**, 131–136 (2018).

33. Cioce, A., Malaker, S. A. & Schumann, B. Generating orthogonal glycosyltransferase and nucleotide sugar pairs as next-generation glycobiology tools. *Curr. Opin. Chem. Biol.* **60**, 66–78 (2021).

34. Malaker, S. A. *et al.* The mucin-selective protease StcE enables molecular and functional analysis of human cancer-associated mucins. *Proc. Natl. Acad. Sci. U. S. A.* **116**, 7278–7287 (2019).

35. Woo, C. M., Iavarone, A. T., Spiciarich, D. R., Palaniappan, K. K. & Bertozzi, C. R. Isotope-targeted glycoproteomics (IsoTaG): a mass-independent platform for intact N- and O-glycopeptide discovery and analysis. *Nat. Methods* **12**, 561–567 (2015).

36. Miyamoto, D. K., Flaxman, H. A., Wu, H. Y., Gao, J. & Woo, C. M. Discovery of a Celecoxib Binding Site on Prostaglandin e Synthase (PTGES) with a Cleavable Chelation-Assisted Biotin Probe. *ACS Chem. Biol.* **14**, 2527–2532 (2019).

37. Calle, B. *et al.* Benefits of Chemical Sugar Modifications Introduced by Click Chemistry for Glycoproteomic Analyses. *J. Am. Soc. Mass Spectrom.* **32**, 2366–2375 (2021).

38. Wei, W. *et al.* Cell type-selective secretome profiling in vivo. *Nat. Chem. Biol.* **17**, 326-334 (2021).

39. Alvarez-Castelao, B. *et al.* Cell-type-specific metabolic labeling of nascent proteomes in vivo. *Nat. Biotechnol.* **35**, 1196–1201 (2017).

40. Xie, R. *et al.* Cell-Selective Metabolic Glycan Labeling Based on Ligand-Targeted Liposomes. *J. Am. Chem. Soc.* **134**, 9914-9917 (2012).

41. Fan, X. *et al.* Cell-type-specific labeling and profiling of glycans in living mice. *Nat. Chem. Biol.* **18**, 625-633 (2022).

42. Mátés, L. *et al.* Molecular evolution of a novel hyperactive Sleeping Beauty transposase enables robust stable gene transfer in vertebrates. *Nat. Genet.* **41**, 753–761 (2009).

43. Kowarz, E., Löscher, D. & Marschalek, R. Optimized Sleeping Beauty transposons rapidly generate stable transgenic cell lines. *Biotechnol. J.* **10**, 647–653 (2015).

44. Shim, M. K. *et al.* Cathepsin B-Specific Metabolic Precursor for In Vivo Tumor-Specific Fluorescence Imaging. *Angew. Chem. Int. Ed.* **55**, 14698–14703 (2016).

45. Shim, M. K. *et al.* Caspase-3/-7-Specific Metabolic Precursor for Bioorthogonal Tracking of Tumor Apoptosis. *Sci. Rep.* **7**, 1–15 (2017).

46. Wang, H. *et al.* Selective in vivo metabolic cell-labeling-mediated cancer targeting. *Nat. Chem. Biol.* **13**, 415–424 (2017).